

# UC Santa Barbara

## UC Santa Barbara Previously Published Works

### Title

Compact broadband polarizer based on shallowly-etched silicon-on-insulator ridge optical waveguides

### Permalink

<https://escholarship.org/uc/item/959523wq>

### Journal

Optics Express, 18

### Authors

Dai, Daoxin  
Wang, Zhi  
Julian, Nicholas  
et al.

### Publication Date

2010-12-14

Peer reviewed

# Compact broadband polarizer based on shallowly-etched silicon-on-insulator ridge optical waveguides

Daoxin Dai,\* Zhi Wang, Nick Julian and John E. Bowers

University of California Santa Barbara, ECE Department, Santa Barbara, CA 93106, USA

\*dx dai@ece.ucsb.edu

**Abstract:** A new way to make broadband polarizers on silicon-on-insulator (SOI) waveguides is proposed, analyzed and characterized. The characteristics of the eigenmodes in a shallowly-etched SOI ridge optical waveguide are analyzed by using a full-vectorial finite-difference method (FV-FDM) mode solver. The theoretical calculation shows that the loss of TE fundamental mode could be made very low while at the same time the TM fundamental mode has very large leakage loss, which is strongly dependent on the trench width. The leakage loss of the TM fundamental mode changes quasi-periodically as the trench width  $w_{tr}$  varies. The formula of the period  $\Delta w_{tr}$  is given. By utilizing the huge polarization dependent loss of this kind of waveguide, a compact and simple optical polarizer based on a straight waveguide was demonstrated. The polarizer is fabricated on a 700nm-thick SOI wafer and then characterized by using a free-space optical system. The measured extinction ratio is as high as 25dB over a 100nm wavelength range for a 1mm-long polarizer.

©2010 Optical Society of America

OCIS codes: (230.7390) Waveguides, planar; (230.5440) Polarization-sensitive devices.

---

## References and links

1. Y. Kokubun, and S. Asakawa, "ARROW-type polarizer utilizing form birefringence in multilayer first cladding," *IEEE Photon. Technol. Lett.* **5**(12), 1418–1420 (1993).
2. L. Pierantoni, A. Massaro, and T. Rozzi, "Accurate modeling of TE/TM propagation and losses of integrated optical polarizer," *IEEE Trans. Microw. Theory Tech.* **53**(6), 1856–1862 (2005).
3. M. A. Duguay, Y. Kokubun, T. L. Koch, and L. Pfeiffer, "Antiresonant reflecting optical waveguides in SiO<sub>2</sub>-Si multilayer structures," *Appl. Phys. Lett.* **49**(1), 13–15 (1986).
4. T. Yamazaki, J. Yamauchi, and H. Nakano, "A branch-type TE/TM wave splitter using a light-guiding metal line," *J. Lightwave Technol.* **25**(3), 922–928 (2007).
5. L. Z. Sun, and G. L. Yip, "Analysis of metal-clad optical waveguide polarizers by the vector beam propagation method," *Appl. Opt.* **33**(6), 1047–1050 (1994).
6. G. Y. Li, and A. S. Xu, "Analysis of the TE-pass or TM-pass metal-clad polarizer with a resonant buffer layer," *J. Lightwave Technol.* **26**(10), 1234–1241 (2008).
7. R. Wan, F. Liu, X. Tang, Y. Huang, and J. Peng, "Vertical coupling between short range surface plasmon polariton mode and dielectric waveguide mode," *Appl. Phys. Lett.* **94**(14), 141104 (2009).
8. R.-C. Twu, C.-C. Huang, and W.-S. Wang, "TE-pass Zn-diffused LiNbO<sub>3</sub> waveguide polarizer," *Microw. Opt. Technol. Lett.* **48**(11), 2312–2314 (2006).
9. Y. Cui, Q. Wu, E. Schonbrun, M. Tinker, J.-B. Lee, and W. Park, "Silicon-based 2-D slab photonic crystal tm polarizer at telecommunication wavelength," *IEEE Photon. Technol. Lett.* **20**(8), 641–643 (2008).
10. A. d'Alessandro, B. Bellini, D. Donisi, R. Beccherelli, and R. Asquini, "Nematic Liquid Crystal Optical Channel Waveguides on Silicon," *IEEE J. Quantum Electron.* **42**(10), 1084–1090 (2006).
11. D. Liang, and J. E. Bowers, "Recent progress in lasers on silicon," *Nat. Photonics* **4**(8), 511–517 (2010).
12. Q. Wang, and S. T. Ho, "Ultra-compact TM-pass silicon nanophotonic waveguide polarizer and design," *IEEE J. Photon.* **2**(1), 49–56 (2010).
13. A. A. Oliner, S. T. Peng, T. I. Hsu, and A. Sanchez, "Guidance and leakage properties of a class of open dielectric waveguides: Part II-New physical effects," *IEEE Trans. Microw. Theory Tech.* **29**(9), 855–869 (1981).
14. K. Ogusu, "Optical strip waveguide: a detailed analysis including leaky modes," *J. Opt. Soc. Am.* **73**(3), 353–357 (1983).
15. M. A. Webster, R. M. Pafchek, A. Mitchell, and T. L. Koch, "Width dependence of inherent tm-mode lateral leakage loss in silicon-on-insulator ridge waveguides," *IEEE Photon. Technol. Lett.* **19**(6), 429–431 (2007).

## 1. Introduction

Polarization multiplexing and demultiplexing are important in photonic integrated circuits (PICs) for fiber optic communication, optical sensing, and optical signal processing. The devices used for polarization handling include polarization beam splitters, polarization rotators, and polarizers. Conventional bulk polarizers are usually based on a birefringent bulk crystal, however, an integrated waveguide polarizer is needed for PICs and, various waveguide polarizers have been developed. The basic principle of the polarizer is to make one polarization more lossy than the other one. In order to have such polarization dependent loss (leakage losses or absorption losses), a waveguide with birefringent materials or structures is used. In Ref [1-3], an antiresonant reflecting optical waveguide (ARROW) structure is used for realizing a polarizer. In the ARROW structure, the radiation loss of TM polarization is over 50dB/cm higher than TE polarization. However, this type of polarizer is usually long (~1cm) and the fabrication is relatively complex because an additional thin high-index cladding is needed. Metal is also often used to realize a polarizer because the strong polarization dependence of the plasmonic modes in a metal-dielectric waveguide [4–6]. In ref [7], a TE-pass polarizer is presented by utilizing the vertical coupling between short range surface plasmon polariton mode and dielectric waveguide mode. The theoretical calculation shows that it possible to realize a high extinction ratio of 30dB and a low loss of 0.1dB by using a rather short length of 50 $\mu$ m. However, this type of polarizer is sensitive to the dimensional variations and the wavelength shift. In ref [8], a TE-pass waveguide polarizer is realized by utilizing the process-dependence characteristics of Zn-diffused waveguides on a y-cut, x-propagation LiNbO<sub>3</sub> substrate at 1.55- $\mu$ m wavelength. The best polarization extinction ratio of 32dB/cm and the corresponding propagation loss of 0.9dB/cm were obtained. In ref [9], a photonic-crystal type polarizer is demonstrated for the 1550nm wavelength. The transmission loss of the TE light was found to be 45 dB, while that of the TM polarized light is as large as 4.5 dB. Liquid crystals (LC) are also often used to realize a polarizer due to the dependence of the transmission loss on the orientation of the LC molecules [10]. By using E7 nematic liquid crystal (LC) in SiO<sub>2</sub>-Si V-grooves [10], a polarizer with an extinction ratio about 25 dB was demonstrated. However, the fabrication and the package become complicated when LC is introduced and the temperature range is limited.

A low-cost and CMOS-compatible polarizer that is compatible with silicon sources and detectors [11] is needed. In ref [12], an ultracompact TM-pass silicon nanophotonic waveguide polarizer was designed. In this paper, we propose and demonstrate a pure silicon TE-passed polarizer based on a shallowly-etched straight optical waveguide. Our polarizer has a very broad wavelength range, which is important for many applications. By optimally designing the shallowly-etched straight optical waveguide, the polarization dependent loss is maximized and consequently a compact polarizer with high extinction ratio is achieved.

## 2. Characteristic analysis for the shallowly-etched SOI ridge waveguide

Figure 1 shows the cross section of optical waveguide used for the proposed polarizer. Here we use a silicon-on-insulator (SOI) wafer, a key element in most platforms for silicon photonics. For the present case, the optical waveguide is defined with two trenches and the etching depth,  $h_r$ , is shallow, e.g.,  $h_r = 0.15H \sim 0.25H$ , where  $H$  is the total height of the Si layer and we choose  $H = 700$ nm for our case for compatibility with low loss waveguides and hybrid silicon lasers and modulators. The refractive indices of silicon and SiO<sub>2</sub> are  $n_{\text{Si}} = 3.455$ ,  $n_{\text{SiO}_2} = 1.445$ , respectively. We use a full-vectorial finite-difference method (FV-FDM) mode solver with the perfect-matched layer (PML) boundary condition. With the FV-FDM mode solver, we can obtain the mode field profile and the propagation constant for all eigenmodes. The leakage loss is calculated with the formula  $L_p = 20\log_{10}[\exp(-n_{\text{im}}k_0l_0)]$ , where  $n_{\text{im}}$  is the imaginary part of the effective index for the fundamental mode,  $k_0$  is the wave number in vacuum ( $k_0 = 2\pi/\lambda_0$ ), and  $l_0$  is the device length (here  $l_0 = 1$ mm).

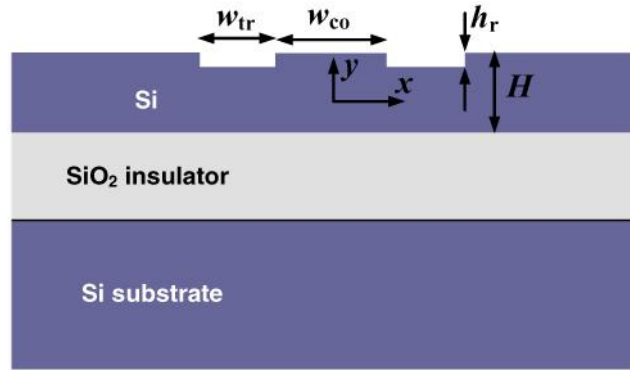


Fig. 1. The cross section of a shallowly-etched SOI ridge waveguide defined by two trenches.

First we consider the case of  $h_r = 140\text{nm}$  and  $w_{co} = 0.8\mu\text{m}$  as an example to show the mode properties of the shallowly-etch SOI ridge waveguide. Figure 2(a)-2(b) show the calculated effective index and the leakage loss for the three eigenmodes with lowest losses as the trench width  $w_{tr}$  ranges from  $2\mu\text{m}$  to  $7\mu\text{m}$ . In such a shallow SOI ridge waveguide, the TE fundamental mode ( $\text{TE}_0$ ) has a dominant electric component  $E_x$ , which can be seen from the field distribution given in Fig. 3 below. This makes it easy to distinguish the  $\text{TE}_0$  mode from the other eigenmodes. However, the situation becomes very different when considering the TM fundamental mode ( $\text{TM}_0$ ) because of mode hybridization. For such hybridized modes, the two transverse components ( $E_x$  and  $E_y$ ) of the electric field are comparable, which makes the  $\text{TM}_0$  mode very similar to a higher order TE mode. In order to distinguish the  $\text{TM}_0$  mode and the higher order TE modes conveniently, we defined the  $\text{TM}_0$  mode as that mode which has larger  $E_y$ -component (i.e.,  $P = \int |E_y|^2 dx dy$ , where the integration region is the ridge region).

From Fig. 2(a), the TE fundamental mode behaves like that of a regular optical waveguide. It can be seen that the effective index of the  $\text{TE}_0$  mode does not change much as the trench width  $w_{tr}$  varies. This is because the  $\text{TE}_0$  mode is confined well in the rib region. On the other hand, the leakage loss increases slightly as the trench width decreases, which is easy to understand by making the ridge waveguide equivalent into a multi-layer slab waveguide, which includes two low-index claddings (corresponding to the trench regions), a core layer (corresponding to the ridge regions), and two outermost layers with the same index as the core. When the low-index cladding is not thick enough, the waveguide becomes leaky. This leakage loss decreases exponentially as the low-index claddings become thick.

For the TM fundamental modes, however, the mode property becomes very different, as shown in Fig. 2(a)-2(b). As the trench width varies, the conversion between the TM fundamental mode and the higher order TE mode happens at some specific range of the trench width as denoted by the green circles in Fig. 2(a). In these ranges, the effective indices as well as the loss for these two modes (i.e., the TM fundamental mode and the higher order TE mode) become very similar. This phenomena looks like quasi-degeneracy of modes. From the leakage losses shown in Fig. 2(b), one sees that there are several peaks for the TM fundamental mode and correspondingly there are several dips at the same position for the higher order TE mode. The trench widths for peaks (or dips) are the same as those for the mode conversion denoted by the circles in Fig. 2(b).

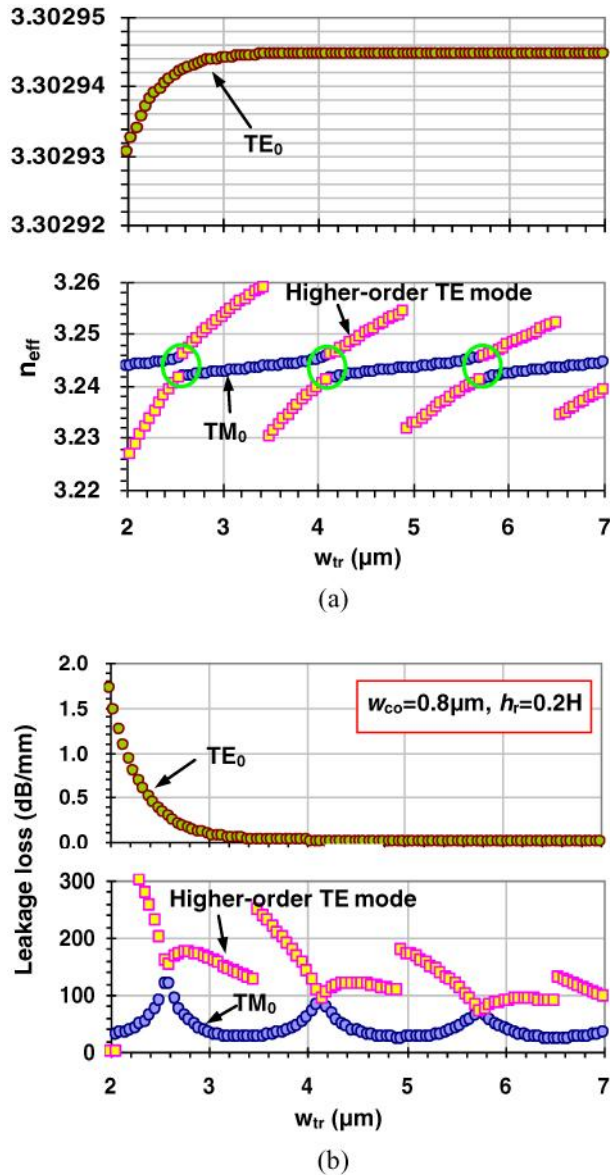


Fig. 2. The effective refractive index of the three eigenmodes (a), and the leakage loss for of the lowest three order eigenmodes (b), as a function of trench width.

In order to see the mode evolution in the shallowly-etched SOI ridge waveguide more clearly, we show the electric field profiles of both components ( $E_x$  and  $E_y$ ) for three modes (including the  $TE_0$ ,  $TM_0$  modes, and the higher order TE mode) in Fig. 3(a)-(c) and Fig. 4(a)-(c). Here we choose two specific trench widths (i.e.,  $w_{tr} = 3.2$ , and  $4.15 \mu\text{m}$ ) because the  $TM_0$  fundamental modes for the cases of  $w_{tr} = 3.2$  and  $4.15 \mu\text{m}$  have local minimal and maximal leakage losses, respectively (as shown in Fig. 2(b)). From Fig. 3(a) and Fig. 4(a), one sees that the  $TE_0$  mode for  $w_{tr} = 3.2$  or  $4.15 \mu\text{m}$  is similar to the regular one, which has a dominant  $x$ -component ( $E_x$ ) and a minor  $y$ -component ( $E_y$ ). However, for the  $TM_0$  fundamental mode ( $TM_0$ ) and the higher order TE mode, the mode profiles become very different as discussed above. From the mode profiles shown in Fig. 3(b) and 3(c), one sees that  $TM_0$  and the higher order TE mode are very similar when the trench width is chosen to be around the peaks of the

leakage loss (e.g.,  $w_{tr} = 4.15\mu\text{m}$  here). This is the phenomenon of mode quasi-degeneracy. In this case, both the  $\text{TM}_0$  mode and the higher order TE mode have significant  $x$ -component as well as  $y$ -component. When the trench width is chosen to be deviated from the peaks (e.g.,  $w_{tr} = 3.2\mu\text{m}$ ), one could see the difference between the  $\text{TM}_0$  mode and the higher order TE mode more easily. For the  $\text{TM}_0$  mode the  $y$ -component becomes dominant while the  $y$ -component for the higher order TE mode is minor. One should note that the minor components for the  $\text{TM}_0$  mode and the higher order TE mode are still significant. Such mode hybridization is due to the TE-TM coupling at the strip boundaries. According to the analysis given in [13–15], the TE-TM coupling will result in significant leakage loss in a rib waveguide. Recently it has also been demonstrated that the TM polarization mode in an ultra-thin SOI ridge waveguide ( $\sim 200\text{nm}$  thick) shows width-dependent leakage loss [15]. For the SOI ridge waveguide considered in this paper, a similar phenomenon is also observed, i.e., the TM polarization has significant leakage loss as shown in Fig. 2(b).

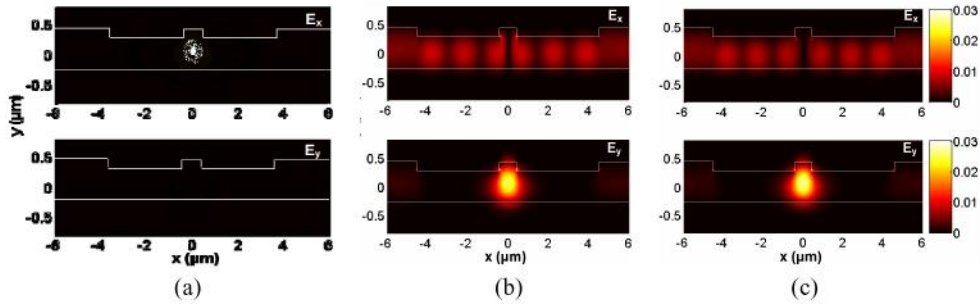


Fig. 3. The mode profiles when  $w_{tr} = 4.15\mu\text{m}$ ,  $h_r = 140\text{nm}$  and  $w_{co} = 0.8\mu\text{m}$ ; (a)  $\text{TE}_0$ ; (b)  $\text{TM}_0$ ; (c) the higher order TE mode.

In the examples shown above, the ridge height is chosen as  $h_r = 140\text{nm}$ . In order to investigate the influence of the ridge height on the leakage loss, we also calculate the eigenmodes ( $\text{TE}_0$  and  $\text{TM}_0$ ) for the cases with different ridge heights ( $h_r = 110$ , and  $140\text{nm}$ ), as shown in Fig. 5(a)-5(b). For any given ridge width  $w_{co}$  and trench width  $w_{tr}$ , the  $\text{TE}_0$  mode has a smaller leakage loss when choosing a larger ridge height  $h_r$ . One could also reduce the leakage loss for the  $\text{TE}_0$  mode by choosing a wider trench width or ridge width. This is because larger height or width of the ridge introduces stronger optical confinement.

For the  $\text{TM}_0$  mode, one sees very different results shown in Fig. 5(a)-(b). For a given core width, the leakage loss changes quasi-periodically as the trench width varies and there are several specific trench widths  $w_{trj}$  to have a local maximal leakage loss. For the waveguide with a larger core width  $w_{co}$  or a larger etch depth  $h_r$ , the quasi-period becomes larger. For the case that the etching depth is very shallow (e.g.,  $h_r \sim 110\text{nm}$ , or  $140\text{nm}$ ), the maximal leakage loss is close to  $120\text{dB/mm}$  when choosing the trench width and the core width appropriately. When a low leakage loss is desired for the TM fundamental mode, one should choose a larger height and width for the rib. The quasi-periodical behavior for the leakage loss shown in Fig. 5(a)-(b) can be explained as follows.

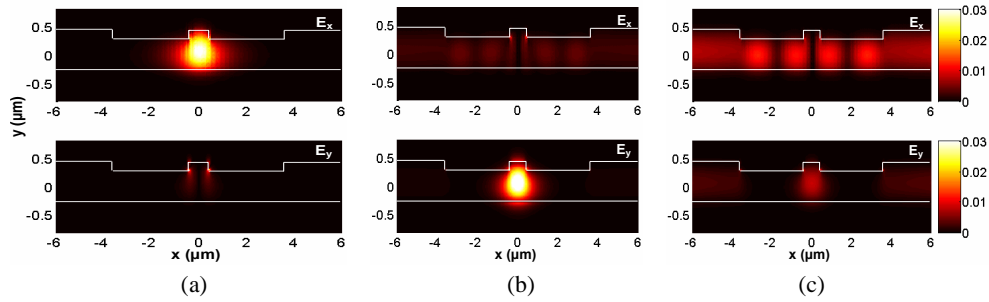


Fig. 4. The mode profiles when  $w_{tr} = 3.2\mu\text{m}$ ,  $h_r = 140\text{nm}$  and  $w_{co} = 0.8\mu\text{m}$ ; (a)  $\text{TE}_0$ ; (b)  $\text{TM}_0$ ; (c) the higher order TE mode.

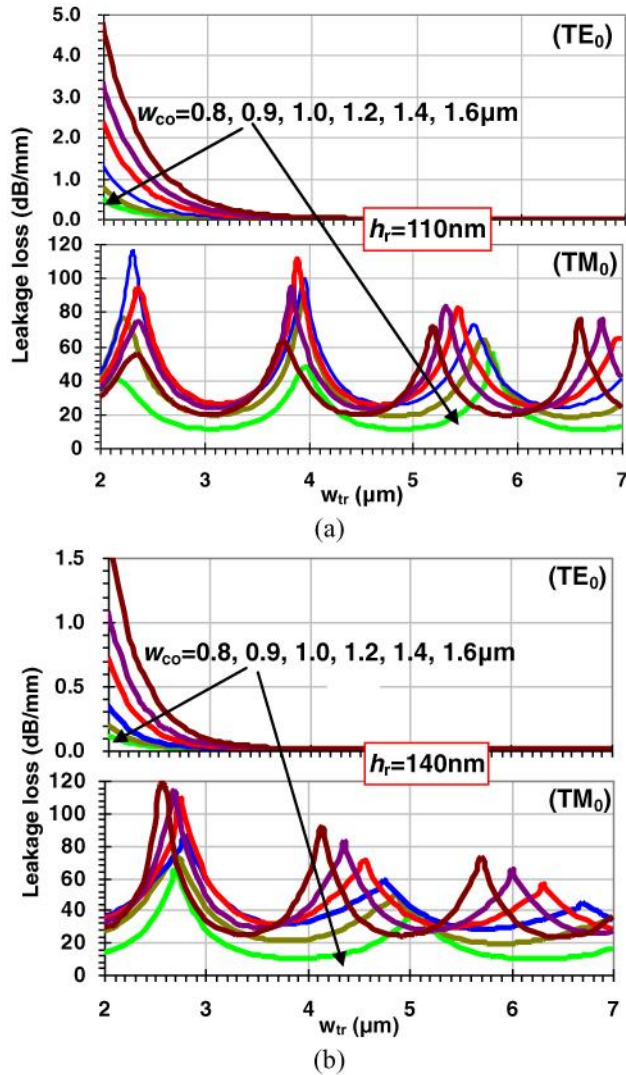


Fig. 5. The leakage losses of the  $\text{TE}_0$  mode and the  $\text{TM}_0$  mode for the cases of  $w_{co} = 0.8, 0.9, 1.0, 1.2, 1.4,$  and  $1.6\mu\text{m}$  as the trench width  $w_{tr}$  varies. (a)  $h_r = 110\text{nm}$ ; (b)  $h_r = 140\text{nm}$ .



As mentioned above, a simple analysis is possible if the ridge waveguide is analyzed as a multi-layer slab waveguide consisting of two low-index claddings (corresponding to the trench regions), a core layer (corresponding to the ridge regions), and two outermost layers with the same index as the core, as shown in Fig. 6. In the SOI ridge waveguide, there is a TE-TM coupling at the strip boundaries [13–15]. In the equivalent five-layer slab waveguide, when the light incident to the core-cladding boundary (#1) as shown in Fig. 6, a part of the light will be reflected and the other will be converted into the TE mode and go forward. When the TE light hits boundary #2, it will be reflected again and enter the core region again. This is very similar to the behavior of the light interference in a single-layer thin film. In order to have a minimal loss, the interference should be constructive and thus the phase condition is then given by

$$2\sqrt{n_{\text{cl\_neff\_TE}}^2 - N_{\text{TM}}^2} w_{\text{tr}} k_0 + \phi_2 - \phi_1 = m2\pi, \quad (1)$$

where  $k_0$  is the wavenumber in vacuum ( $k_0 = 2\pi/\lambda$ ),  $n_{\text{cl\_neff\_TE}}$  is the cladding index in the equivalent five-layer slab waveguide for TE mode,  $N_{\text{TM}}$  is the effective index of the SOI ridge waveguide for the TM fundamental mode,  $\phi_1$  and  $\phi_2$  are the phase changes when light is reflected at boundary #1 and #2. This formula is similar to those given in ref [13–15]. From Eq. (1), the period for the trench width shown in Fig. 5(a)-(b) is given by

$$\Delta w_{\text{tr}} = \frac{\lambda}{2\sqrt{n_{\text{cl\_neff\_TE}}^2 - N_{\text{TM}}^2}}, \quad (2)$$

When the core width increases, the effective index  $N_{\text{TM}}$  becomes larger and consequently the denominator in Eq. (2) becomes smaller. Therefore, the period  $\Delta w_{\text{tr}}$  is larger, which is consistent with what is seen in Fig. 5(a)-(b). When the rib height become shallow (i.e., the Si height ( $H-h_r$ ) in the trench region is larger), the effective index  $n_{\text{cl\_neff\_TE}}$  is larger and consequently one has a smaller period  $\Delta w_{\text{tr}}$  (according to Eq. (2)). This is also seen by comparing the results for  $h_r = 110\text{nm}$ , and  $140\text{nm}$  shown in Fig. 5(a)-(b). For example, for the cases of  $h_r = 110\text{nm}$  and  $140\text{nm}$ , the effective index  $N_{\text{TM}}$  is 3.243101 and 3.249885, respectively, and the effective index  $n_{\text{cl\_neff\_TE}}$  is 3.283214 and 3.297138, respectively. Consequently the period  $\Delta w_{\text{tr}}$  calculated by using Eq. (2) are  $1.51\mu\text{m}$  and  $1.39\mu\text{m}$ , which are close to those read from Fig. 5(a)-5(b).

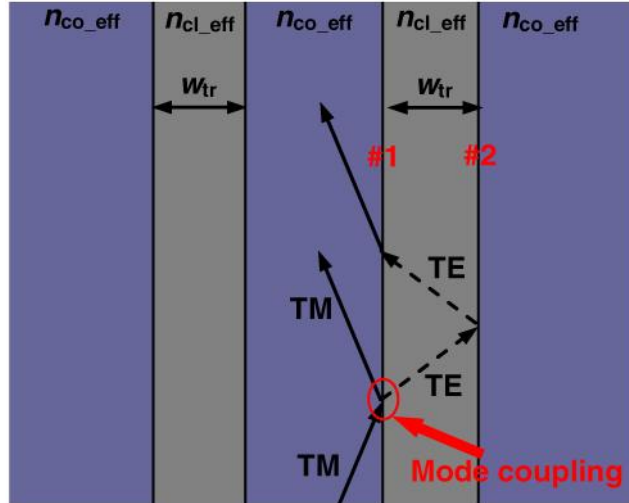


Fig. 6. The equivalent five-layer slab waveguide for the SOI ridge waveguide.



Figure 7(a) and 7(b) show the calculated leakage losses at 1550nm for TE and TM polarizations as the core width  $w_{co}$  ranges from  $3\mu\text{m}$  to  $0.8\mu\text{m}$ . In this calculation, we choose the trench width  $w_{tr} = 2, 3, 4,$  and  $5\mu\text{m}$ . For TE polarization, it can be seen that the leakage loss is very low when choosing a relatively large trench with. For TM polarization, as shown in Fig. 7(b), one sees that the leakage loss increases significantly when the core width decreases to about  $2\mu\text{m}$  or less. The trench width also plays an important role for the leakage loss. According to the mode analyses above, one can realize a polarizer with a high extinction ratio by utilizing the huge polarization dependent loss of the shallowly-etched SOI ridge waveguide. For example, the theoretical extinction ratio is over 60dB when using a 1mm-long straight waveguide with  $w_{tr} = 3\mu\text{m}$  and  $w_{co} = 1.1\mu\text{m}$ .

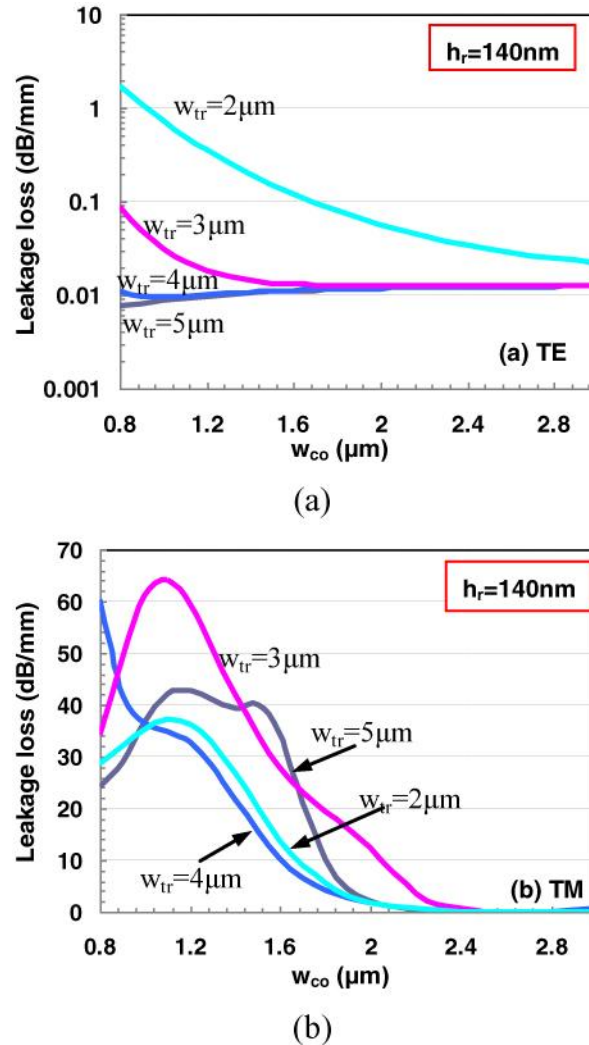


Fig. 7. The leakage loss for TE (a) and TM (b) polarizations for a shallowly-etched SOI ridge waveguide (the rib height  $h_r = 140\text{nm}$ ).

For a polarizer, it is usually desirable to have low loss for the through polarization (e.g., TE polarization for the present case) as well as a compact length. In order to get the optimal design, we consider the requirements of  $L_{TE} < 0.1\text{dB}$  and  $l < 0.1\text{cm}$ , where  $L_{TE}$  is the loss for TE polarization and  $l$  is the length of the polarizer. For the requirement of  $L_{TE} < 0.1\text{dB}$ , the polarizer length  $l$  should satisfy  $l < l_{\max} = 0.1/L_{TE0}$  where is the loss for TE polarization per

unit length (dB/mm). Combining with the condition of  $l < 1\text{mm}$ , the length of the polarizer is then given by  $l = \min(1\text{mm}, 0.1/L_{\text{TE0}})$ . With this length, the extinction ratio of the polarizer is shown in Fig. 8. Theoretically speaking, it is possible to obtain a very high extinction ratio, i.e.,  $>64\text{dB}$  when  $w_{\text{tr}} = 3\mu\text{m}$  and  $w_{\text{co}} = 1.1\mu\text{m}$ . Figure 9 shows the wavelength dependence of the leakage loss for TE and TM polarizations of the designed 1mm-long polarizer with  $w_{\text{tr}} = 3\mu\text{m}$  and  $w_{\text{co}} = 1.1\mu\text{m}$ . One sees that this polarizer has a very broad-band (1450~1650nm) as well as a high extinction ratio ( $>50\text{dB}$ ).

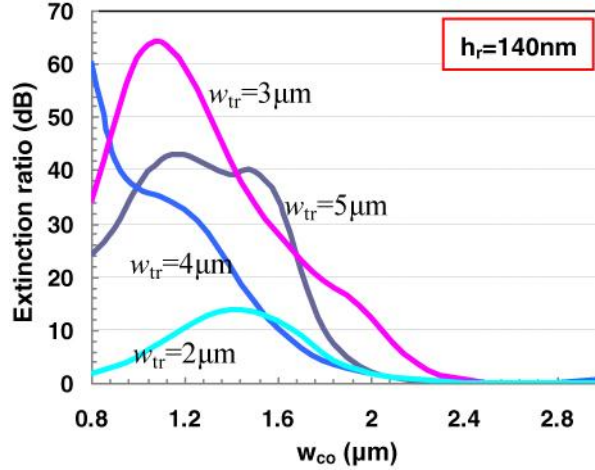


Fig. 8. The extinction ratio for a 1mm-long polarizer with the requirement of  $L_{\text{TE}} \leq 0.1\text{dB}$  and  $l \leq 1\text{mm}$ . Here  $l = \min(1\text{mm}, 0.1/L_{\text{TE0}})$ .

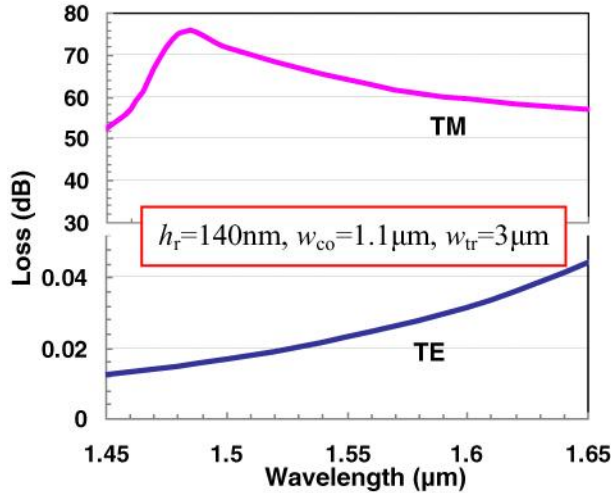


Fig. 9. The wavelength dependence of the leakage loss for TE and TM polarizations for a shallowly-etched SOI ridge waveguide with  $h_r = 140\text{nm}$ ,  $w_{\text{co}} = 1.1\mu\text{m}$ , and  $w_{\text{tr}} = 3\mu\text{m}$ .

### 3. Fabrication and measurement

Figure 10 shows a schematic configuration of the present polarizer, which consists of a straight waveguide defined by two trenches. The two trenches are tapered to be wider at both ends. We use standard processes (including UV lithography, ICP etching, etc.) for the fabrication of the present SOI polarizer. In order to characterize the fabricated devices, we use the measurement setup shown in Fig. 11, which includes a free-space optical system for

polarization-controlling to have a polarized input light with a high extinction ratio. The extinction ratio of input polarized light at the input side is up to 40dB.

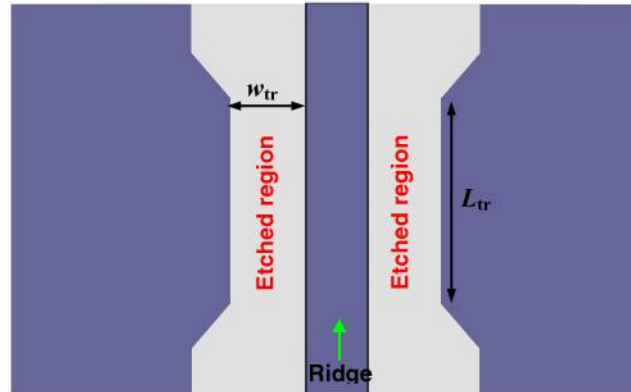


Fig. 10. The schematic configuration of the present SOI polarizer based on a straight waveguide.

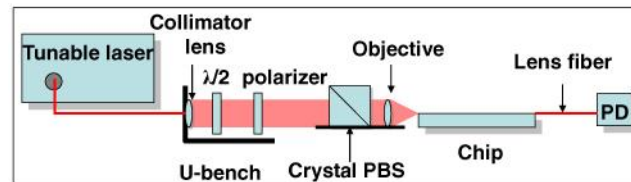
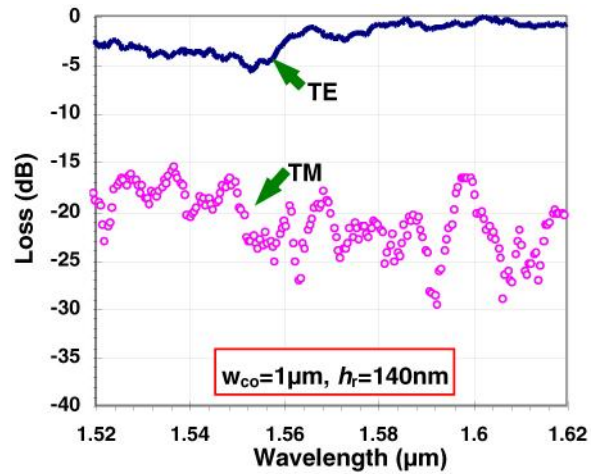
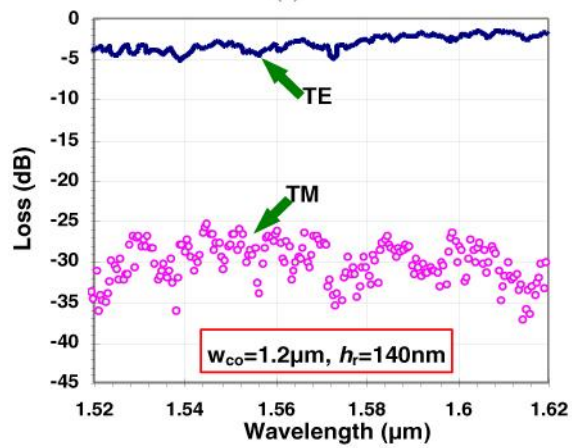


Fig. 11. The measurement setup.

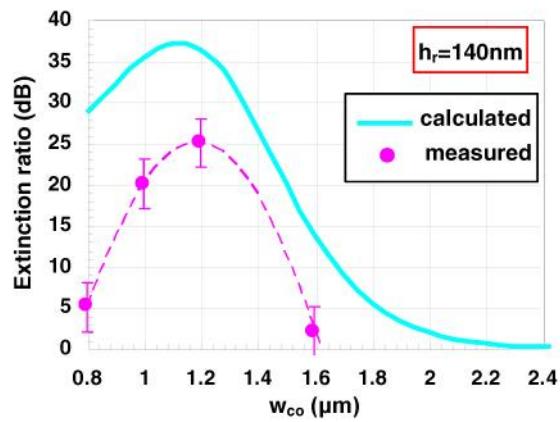
Figure 12(a) and 12(b) show the measurement transmission losses of both TE and TM polarizations for the designs with  $w_{co} = 1.0\mu\text{m}$  and  $1.2\mu\text{m}$ , respectively, and the length  $L_{tr} = 1\text{mm}$ . The trench width is  $w_{tr} = 2.0\mu\text{m}$ . Here the coupling loss is excluded. It can be seen that the loss of the  $\text{TM}_0$  mode is much higher than the  $\text{TE}_0$  mode, as expected from the calculation results shown above. The present polarizer also shows a broad-band response ( $>100\text{nm}$ ). Figure 12(c) shows the extinction ratio for the polarizer with different rib width  $w_{co}$ . The solid curve is the calculation result while the circles are the measured one. It can be seen that they agree well with each other qualitatively. Both the calculation and measurement show that there is a maximal extinction ratio around  $w_{co} = 1.2\mu\text{m}$ . The measured extinction ratio is lower than the calculated one, which might be because TE polarization has higher scattering than expected. Another possible reason is that TM polarization has some background noise due to the scattering when the TM light leaks and touches the adjacent waveguides in the same wafer.



(a)



(b)



(c)

Fig. 12. The measured results for the transmissions of the  $\text{TE}_0$  and  $\text{TM}_0$  modes when  $w_{co} = 1 \mu\text{m}$  (a), and  $w_{co} = 1.2 \mu\text{m}$  (b); (c) the extinction ratio. The trench width is  $w_{tr} = 2 \mu\text{m}$  and the length  $L_{tr} = 1 \text{ mm}$ .

#### 4. Conclusion

In this paper, we have given a detailed analysis for the mode characteristics of shallowly-etched silicon-on-insulator ridge optical waveguides by using FV-FDM mode solver with a PML boundary treatment. It has been shown that the leakage loss of the present SOI ridge waveguide is very strongly polarization-dependent. The TE fundamental mode can be low loss while the TM fundamental mode has very large leakage loss. More importantly, the leakage loss of the TM fundamental mode changes quasi-periodically as the trench width  $w_{tr}$  varies. The formula of the period  $\Delta w_{tr}$  is also given. By utilizing the huge polarization dependent loss of this kind of waveguide, we have proposed a compact and simple optical polarizer based on a straight waveguide. The large dependence of the TM leakage loss on the trench width indicates that one has to choose the trench width optimally to have a maximal extinction ratio. Both the theoretical and experimental results show that the proposed polarizer has very broad bandwidth. The measured extinction ratio is as high as 25dB over a 100nm wavelength range for a 1mm-long polarizer.

#### Acknowledgments

This work was supported by DARPA MTO under the CIPhER contract HR0011-10-1-0079.